Reprinted from JOURNAL OF SPACECRAFT AND ROCKETS, Vol. 10, No. 3, March 1973, pp. 175-180

Theoretical, Quasi-Static Analysis of Cavitation Compliance in Turbopumps

C. BRENNEN* AND A. J. ACOSTA†
California Institute of Technology, Pasadena, Calif.

The serious POGO instability experienced by many liquid propellant rockets results from a closed loop interaction between the first longitudinal structural mode of vibration and the dynamics of the propulsion system. One of the most important features in the latter is the cavitation compliance of the turbopumps. This report presents calculations of the blade cavitation compliance obtained from free streamline cascade theory and demonstrates the various influences of angle of attack, blade angle, blade thickness and cavitation number. Discrepancies between calculated and experimentally derived values are discussed.

Nomenclature

A	= real constant
A_i	= inducer inlet area
B	= real constant
C_B	= dimensional cavitation compliance of the turbopump
d	= blade thickness
f	= frequency
h	= distance between the leading edges of the blades
H	= tip blade spacing, $(h)_{r=R}$
K^*	= cascade and local dimensionless cavitation compliance $= -\partial v^*/\partial\sigma$
K_T^*	= local dimensionless cavitation compliance at blade tip, $(K^*)_{r=R}$
K_B	= over-all dimensionless compliance of turbopump
l	= point corresponding to cavity closure in ζ plane
l_c	= cavity length
p_s	= upstream static pressure
p_c	= cavity pressure
r	= radial coordinate at inducer inlet
R	= blade tip radius
R_H	= inducer hub radius
u,v	= velocity components in the x,y directions
v^*	$= V^*/h^2$
V	= total volume of cavities in the inducer
V_1	= magnitude of upstream fluid velocity relative to the blades
V_2	= magnitude of downstream fluid velocity
V_c	= magnitude of cavity surface velocity
V_T	= tip fluid velocity, $(V_1)_{r=R}$
V^*	= cascade cavity volume per unit depth of flow
w	$= u - iv$
x,y	= coordinates parallel and perpendicular to the cascade
y_B	= foil profile
y_c	= cavity profile above the foil
z	$= x + iy$
Z	= number of inducer blades
α	= angle of attack
β	= blade angle
$\zeta = \xi + i\eta$	= complex variable in the transformed plane
ζ_1	= point corresponding to upstream infinity in ζ plane
$\bar{\zeta}_1$	= complex conjugate of ζ_1
ρ	= liquid density
σ	= cavitation number, $\sigma = (p_s - p_c)/\frac{1}{2}\rho V_1^2$
σ_C	= choked cavitation number
σ_L	= local cavitation number at a position, r
σ_T	= tip cavitation number at $r = R$
σ_{CT}	= choked tip cavitation number
ω	= reduced frequency

Introduction

DURING the first or booster stage of flight many liquid propellant rockets have experienced severe longitudinal vibrations caused by a closed loop interaction between the first longitudinal structual mode and the dynamics of the propulsion system. This, POGO instability,[1] has been the subject of intensive research since it was first encountered. One of the most important transients in the dynamic modelling of the propulsion system is the cavitation compliance of the turbopumps,[2] C_B, defined as the rate of change of the mass of propellant within the pump with respect to the inlet or suction pressure, p_s. When the pump is cavitating it follows that

$$C_B = -\rho\, \partial V/\partial p_s \tag{1}$$

Thus the compliance describes the oscillatory source/sink behavior of the pump due to fluctuating cavity volumes. Past analyses such as those of Ghahremani[3] have suggested dividing this compliance into two components corresponding to the two major types of pump cavitation, namely blade cavitation and backflow cavitation.

The purpose of this paper is to present some theoretical calculations of blade cavitation compliance obtained using cascade analysis. The usual philosophy behind such analyses involves considering the flow through every axisymmetric annular section of the inducer or impeller as being modelled by a planar cascade flow such as that sketched in Fig. 1. Then the most satisfactory starting point would be a theory for oscillatory flow through a cascade with finite, fluctuating cavities. Unfortunately no such theory has, as yet, been completed. The present paper explores the quasistatic or low frequency approach by employing modifications of existing steady flow theory for cavitating cascades. Comment on the validity of such an approximation in typical turbopump operation is presented in the comparison with experiment section.

Linearized Theory for Cavitating Cascades

Free streamline potential flow models of a cavitating cascade have been employed extensively in the past to study blade cavitation in turbomachinery. Most of the methods have been based on a linearized approach[4-7] though Stripling and Acosta[8] also consider the nonlinear problem. However, virtually all of these solutions represent the blades as being infinitely thin, thus neglecting the important effects of finite leading edge curvature and finite blade thickness. The present theory attempts to include these effects through a modification of the simple solution of Acosta and Hollander[4] for the flow through a cascade of infinitely long foils with partial cavitities (as shown in Fig. 1 where the

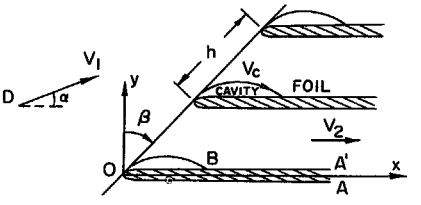

Fig. 1 Physical plane ($z = x + iy$) of the cascade.

Received July 12, 1972; revision received October 24, 1972. This work was carried out under NASA Contract NAS8-28046.
Index categories: Liquid Rocket Engines; Multiphase Flows; Hydrodynamics.

* Senior Research Fellow in Engineering Science.
† Professor of Mechanical Engineering.

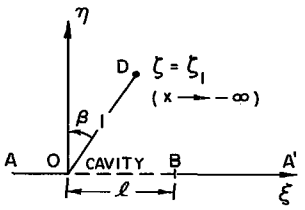

Fig. 2 The transformed plane ($\zeta = \xi + i\eta$).

symbols used below are defined). This geometry is then conformally mapped into the ζ-plane of Fig. 2 by

$$2\pi(z/h) = e^{-i\beta}\ln(1 - \zeta/\zeta_1) + e^{i\beta}\ln(1 - \zeta/\bar{\zeta}_1) \quad (2)$$

With the conventional linearization and infinitely thin blades, Acosta and Hollander were then able to write down the solution for $w(\zeta) = u - iv$ by inspection as

$$w(\zeta)/V_1 = B[\zeta/(\zeta - l)]^{1/2} - A[(\zeta - l)/\zeta]^{1/2} + V_c/V_1 \quad (3)$$

where A, B are real constants determined by the conditions at upstream and downstream infinity. Further, from the definition of cavitation number, it follows that $V_c/V_1 = (1 + \sigma)^{1/2}$.

The present authors, however, considered the question of how a finite blade thickness might be most easily incorporated into this solution. This was accomplished by the addition of the simple round-nose singular component $-id\cos\beta/\zeta$ (d real) to the expression for $w(\zeta)$; then

$$\frac{w(\zeta)}{V_1} = -\frac{id\cos\beta}{\zeta} + B\left(\frac{\zeta}{\zeta - l}\right)^{1/2} - A\left(\frac{\zeta - l}{\zeta}\right)^{1/2} + (1 + \sigma)^{1/2} \quad (4)$$

The boundary conditions which determine A, B are then 1) at $x \to -\infty$ or $\zeta = \zeta_1 = ie^{-i\beta}$, $w/V_1 = e^{-i\alpha}$ so

$$e^{-i\alpha} = -\frac{id\cos\beta}{\zeta_1} + B\left(\frac{\zeta_1}{\zeta_1 - l}\right)^{1/2} - A\left(\frac{\zeta_1 - l}{\zeta_1}\right)^{1/2} + (1 + \sigma)^{1/2} \quad (5)$$

2) at $x \to +\infty$ or $|\zeta| \to \infty$, $w/V_1 = V_2/V_1$ so

$$V_2/V_1 = B - A + (1 + \sigma)^{1/2} \quad (6)$$

3) a continuity condition between upstream and downstream infinity so that

$$V_2/V_1 = \cos(\alpha + \beta)/(1 - d)\cos\beta \quad (7)$$

Thus the solution and the cavitation number can be rewritten in terms of d, α, β, h, V_1, and the parameter l.

The foil shape and cavity profile must now be determined. The ordinate, y, of a point in the z-plane which corresponds to a point on the real axis, $\eta = 0$, of the ζ-plane is given by

$$y(\xi) = \int_0^x \frac{dy}{dx}\,dx = -\frac{1}{V_1}\,\mathrm{Imag}\left[\int_0^\xi w\frac{dz}{d\zeta}\,d\zeta\right] \quad (8)$$

Outside the interval $0 < \xi < l$ this yields

$$y_B(\xi)/h = \pi^{-1}d\cos\beta\tan^{-1}[\xi\cos\beta/(1 - \xi\sin\beta)] \quad (9)$$

which must therefore represent the foil profile. It will be assumed that the same equation also represents the foil profile within or underneath the cavity. The foil therefore has a parabolic leading edge of radius $d^2\cos^3\beta/\pi$ and tends to finite thickness further downstream, the ratio of the foil thickness/normal spacing of the blades being d. Thus d may be fixed either on the basis of the blade thickness or on the basis of leading edge radius; however these features cannot be varied independently in the present model.

Performing the integral in Eq. (8) within the interval $0 < \xi < l$ demonstrates that the cavity profile is described by an additional ordinate $y_c(\xi)$ on top of the foil profile where

$$\frac{y_c(\xi)}{h} = \frac{1}{\pi}\,\mathrm{Imag}\left(e^{-i\beta}\left[\left\{(1 + \sigma)^{1/2} - \frac{V_2}{V_1}\right\}\ln\left(\frac{1 - \{\xi/(\xi - l)\}^{1/2}}{1 + \{\xi/(\xi - l)\}^{1/2}}\right) + (e^{-i\alpha} - (1 + \sigma)^{1/2} + id\cos\beta/\zeta_1)\times \ln\left(\frac{\{\zeta_1/(\zeta_1 - l)\}^{1/2} - \{\xi/(\xi - l)\}^{1/2}}{\{\zeta_1/(\zeta_1 - l)\}^{1/2} + \{\xi/(\xi - l)\}^{1/2}}\right)\right]\right) \quad (10)$$

The coordinates of the foil and cavity profile are then completely determined parametrically by Eqs (9) and (10) along with the real part of Eq. (2) which gives $x(\xi)/h$.

One slight inconsistency in the solution arises if $y_c(l)$, which should be zero, is evaluated using Eq. (10). Instead it is found that $y_c(l)$ is zero only if $V_1/V_2 = [\cos(\alpha + \beta) + d\cos\beta]/\cos\beta$. When α and d are small this condition is virtually identical with the continuity condition [Eq. (7)] so the inconsistency is very small and proved to be negligible in all the presented data; it is inherent in the linearization effected in Eq. (8).

Numerical integrations were then performed in order to determine the volume of the cavity/unit depth of the plane, V^*. The ratio $v^* = V^*/h^2$ was calculated for various values of α, β, d, and σ. A dimensionless cavitation compliance, K^*, is then given by the derivative $(-\partial v^*/\partial\sigma)$. Sample values with $\alpha = 5°$, $\beta = 75°$ are shown in Fig. 3; note that a) the cavitation number at which the flow is choked increases with foil thickness; b) the compliance tends to infinity in this limit because the cavity becomes infinitely long; c) the unexpected inflexion in the curves occurs at a value of σ at which the closure point of the cavity is roughly opposite the leading edge of the neighboring foil. It was discovered that while the cavity length increases monotonically as σ is reduced, the maximum height, which also increases over most of the range, in fact may decrease as the end of the cavity passes this location on the foil. The net effect on the derivative of the cavity volume will then be of the form illustrated by Fig. 3. Indeed, under some circumstances, K^* may even become negative over a short range of σ; d) eventually as σ becomes very large, K^* tends to zero.

Blade Cavitation Compliance in an Inducer

Values for K^* calculated in the preceding section must now be related to the typical dimensional pump compliance which we would expect to measure. Unfortunately C_B is given dimensions L^2 in the literature; but, from a strict hydrodynamic point of view, the correct dimensions are LT^2 and experimental results presented in the past should be divided by the gravitational acceleration, g, giving units for C_B like $m \times \sec^2$. The appropriate nondimensional version of C_B is therefore not the often used C_B/A_i (A_i being the inducer inlet area) but some other grouping which is determined below.

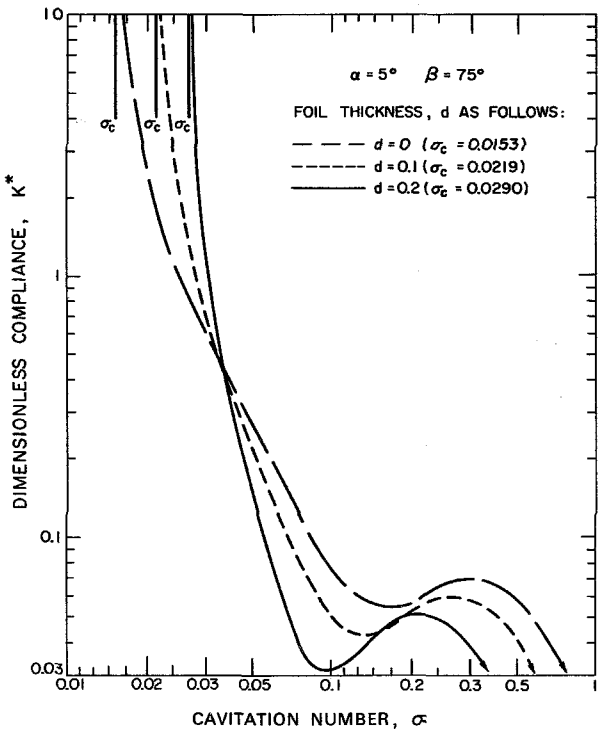

Fig. 3 Typical values of theoretical blade compliance for a cascade.

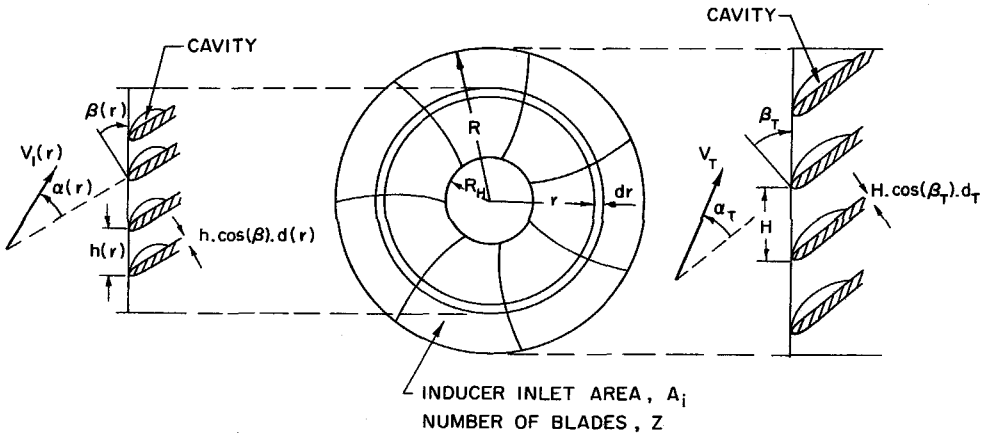

Fig. 4 Inducer inlet section with nomenclature.

Now consider an annulus of depth dr at radius r in the inlet section of the inducer (Fig. 4). In the following approximate treatment, fluid velocity components normal to the axis of the inducer will be neglected so that each annulus can be treated as hydrodynamically separate. Since α, β, and d, will vary with r in some manner to be prescribed in a particular problem, it follows from the preceding section that v^* can be considered as a determinable function of both r and the local cavitation number σ_L where

$$\sigma_L = (p_s - p_c)/\tfrac{1}{2}\rho V_1^2 \tag{11}$$

But V_1 is a known function of r and p_s and p_c are constants; indeed since the component of V_1 due to the rotation of the inducer is usually large compared with the axial fluid velocity, the following relations are sufficiently accurate for present purposes.

$$V_1 \simeq rV_T/R \qquad \sigma_L \simeq R^2\sigma_T/r^2 \tag{12}$$

Conventionally, σ_T is considered as the over-all cavitation number for the pump.

It follows from the definition of v^* that the total cavity volume in the annulus dr is $v^*(\sigma_L,r) \times \{h(r)\}^2 \times Z\,dr$ where $h(r) = 2\pi r/Z$. Then the total cavity volume in the pump is

$$V = \int_{R_H}^{R} v^*(\sigma_L,r) \times \{h(r)\}^2 \times Z\,dr \tag{13}$$

To obtain the compliance C_B note that from Eqs. (11) and (12)

$$\partial/\partial p_s \equiv 2/\rho V_T^2 \cdot (R^2/r^2)(\partial/\partial\sigma_L)$$

It follows that

$$C_B = -\rho\frac{\partial V}{\partial p_s} = \frac{8\pi^2R^2}{V_T^2 \cdot Z}\int_{R_H}^{R}\left\{-\frac{\partial v^*}{\partial\sigma_L}\right\}\cdot dr$$

$$= \frac{4\pi HR^2}{V_T^2}\int_{R_H/R}^{1} K^*(\sigma_L,r/R)\,d\left(\frac{r}{R}\right) \tag{14}$$

where K^* may be calculated by the method of the previous section knowing the local values of α, β, d, and σ_L. Because of the relation [Eq. (12)], K^*, which is dimensionless, can also be regarded as a function only of σ_T and r/R.

For example if it transpired that K^* were linear in r so that $K^*(\sigma_T,r/R) = r/R \cdot K_T^*(\sigma_T)$, then

$$K_T^* = (V_T^2/2HA_i)C_B$$

This demonstrates the correct kind of grouping to be used in nondimensionalizing C_B. Indeed we will define a general over-all, nondimensional compliance, K_B, for the inducer as

$$K_B = \frac{V_T^2}{(2HA_i)}\cdot C_B = \frac{2}{[1-(R_H/R)^2]}\int_{R_H/R}^{1} K^*(\sigma_T,r/R)\,d\left(\frac{r}{R}\right) \tag{15}$$

This choice is based on the observations of the following section in which at least under some conditions, K^* is very roughly proportional to r so that the numerical values of K_B and K_T^* are close to one another.

Theoretical Calculations of Blade Compliance for Saturn Turbopumps

In this and the following sections theoretical calculations and comparison with measured data will be made for the fuel $(-F)$ and oxidizer $(-O)$ pumps of the Saturn booster engines J2, F1, and H1. In this section the radial integration derived in the last section will be applied to the pumps, J2 − 0 and F1 − 0. The approximate radial variation of α, β, d for the inducers of these pumps was taken from Vaage, Fidler, and Zehnle[9] and is presented in Fig. 5. This was used to calculate the dimensionless compliance K^* and the choked cavitation number, σ_C, at six radial stations. The σ_C data was converted to values of the tip or pump cavitation number, σ_{CT} at which the flow at that radial position would be choked using $\sigma_{CT} = r^2\sigma_C/R^2$. The results are shown in Fig. 6. It is especially notable and surprising that as σ_T is reduced the flow should first become choked fairly close to the hub; this is primarily due to the greatly increased blade thickness and angle of attack in this region compared with that at the blade tip.

The practical phenomenon of turbopump breakdown is normally associated with flow choking in the pump and thus it is of interest to compare the theoretical data with the measured pump cavitation numbers at which breakdown occurs. Values of the breakdown cavitation number for J2 − 0 and F1 − 0 when the liquid is LOX and when it is water are quoted by Ghahremani[3]

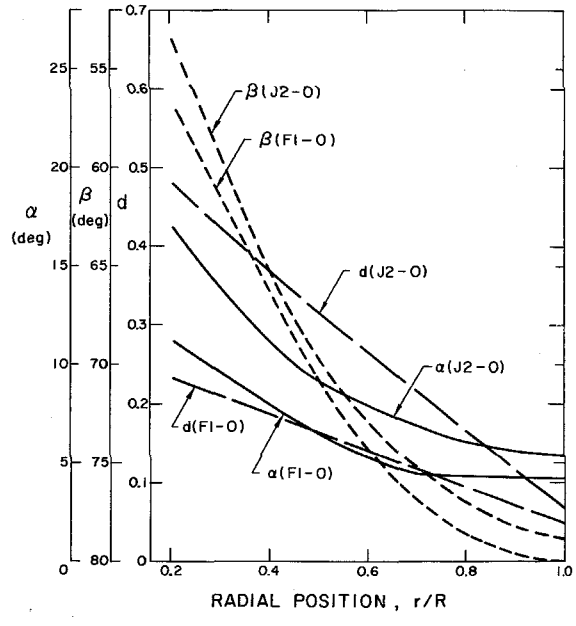

Fig. 5 Radial variation of geometrical parameters for the inducers of J2-0 and F1-0 turbopumps.

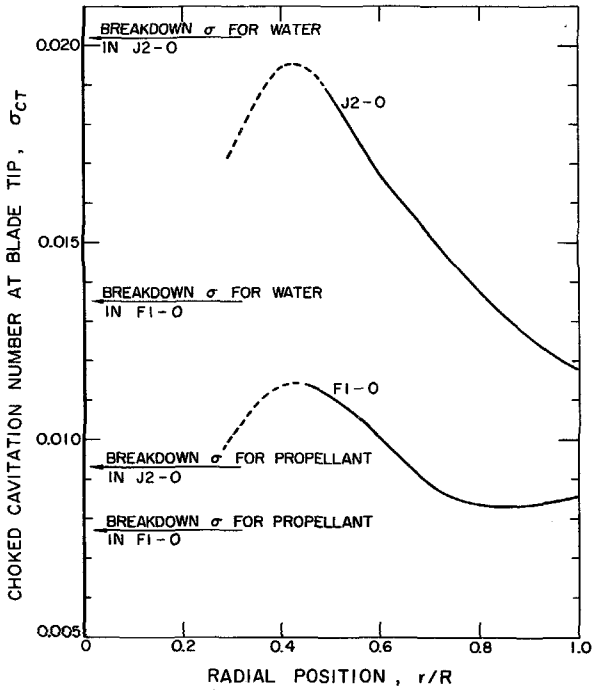

Fig. 6 The tip cavitation number at which the flow at each radial position becomes choked plus experimental breakdown cavitation numbers.

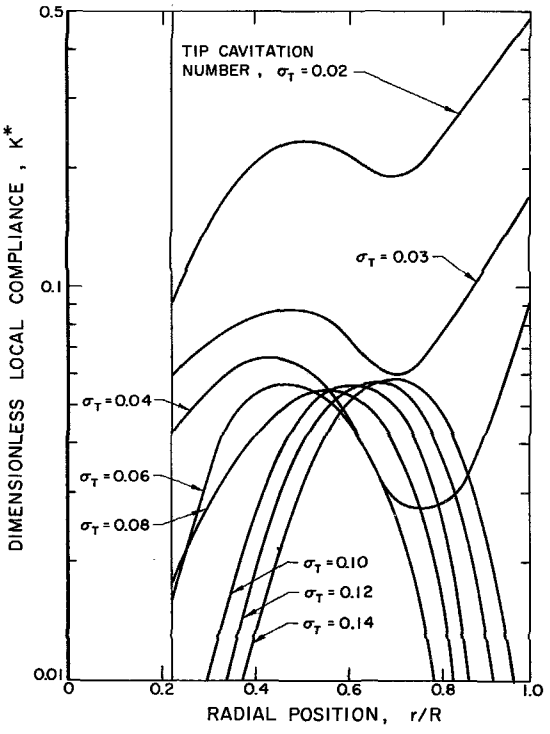

Fig. 8 Radial distribution of compliance for various σ_T in the F1-0 turbopump.

and are included in Fig. 6. It is noteworthy that for both pumps the two values bracket the calculated curves.

The radial distributions of compliance, K^*, are shown in Figs. 7 and 8 for various values of the tip cavitation number, σ_T. Figure 7 shows that K^* for the pump J2 – 0 is very roughly linear in r except at high σ_T but the same cannot be said of the pump F1 – 0. The curves reflect inflexions in the curves of K^* against σ for particular r/R as was discussed in section 2. For example at the blade tip in the case of F1 – 0, the K^* actually becomes negative in the approximate range $0.07 < \sigma_T < 0.11$ (see Fig. 10). However, these inflexions occur for different σ at different r/R so that the radial integration to find K_B shows (see Figs. 9, 10) that the over all compliance exhibits no such marked deviation.

The theoretical values of K_B are presented in Figs. 9, 10 and are then compared with the theoretical local tip compliance K_T^*. The curves demonstrate that the preliminary temptation to equate the theoretical local tip compliance with the pump compliance, K_B, can be effective in some instances but may be misleading in others. Nevertheless, since radial distribution data for other pumps J2 – F, F1 – F, H1 – F, and H1 – 0 was not available, only the local tip compliance, K_T^* has been calculated in these cases (using data given by Vaage, Fidler, and

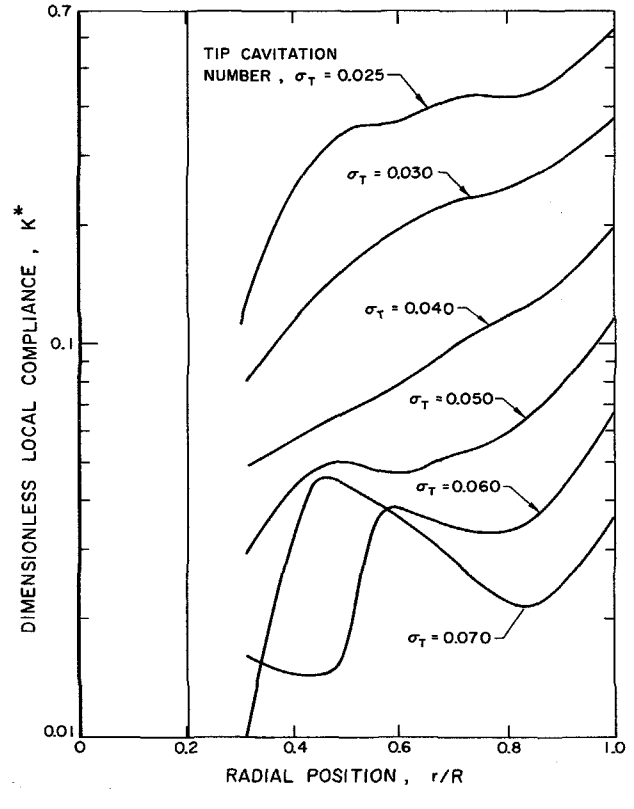

Fig. 7 Radial distributions of compliance for various σ_T in the J2-0 turbopump.

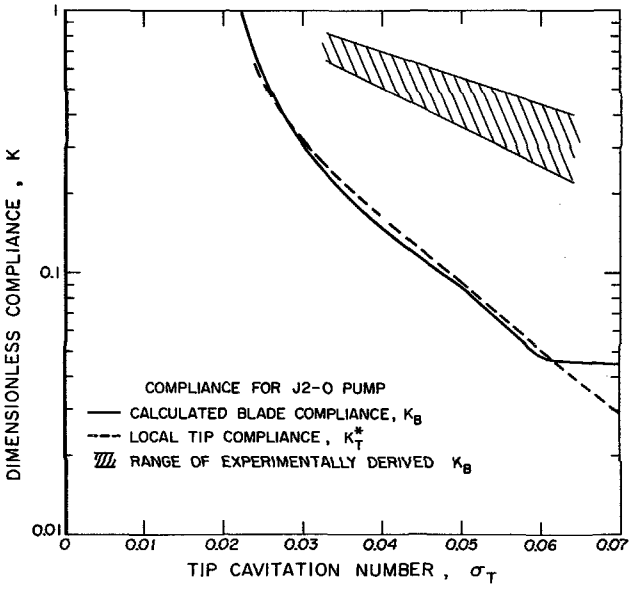

Fig. 9 Compliance for the J2-0 turbopump.

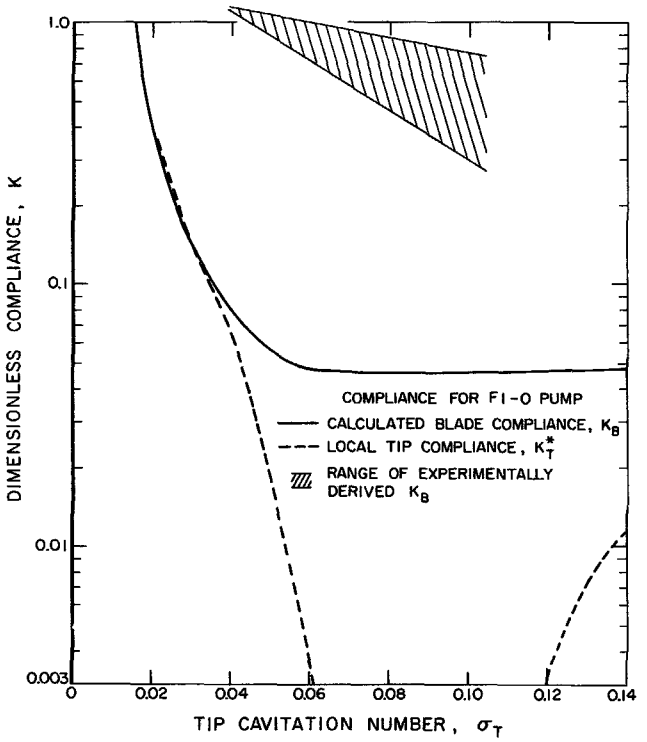

Fig. 10 Compliance for the F1-0 turbopump.

Zehnle[9] and a representative value of $d = 0.1$) and the results are presented in Fig. 11 for the purposes of comparison with experiment.

Comparison with Experiment

Total cavitation compliance values for the pumps of the J2, F1, and H1 Saturn booster engines have been derived from experimental data by Vaage, Fidler, and Zehnle.[9] These are nondimensionalized according to the relation [Eq. (15)] and presented in Figs. 9–11. Unfortunately, these experimental values are by no means direct measurements but are inferred from rather complex dynamic models into which experimental observations are substituted. Much more direct measurements of compliance would clearly be preferable but have not as yet been made; until such time as these become available some doubt must remain concerning the validity of these dynamic models and the experimental values derived from them. In addition, the scatter in these values of the compliance approaches an order of magnitude. Hence some caution must be exercised in interpreting the apparent lack of agreement between the experimental values of total compliance and the present theoretical values of blade compliance in Figs. 9–11. Nevertheless it is worth reviewing in some detail the limitations of the present theoretical approach and possible reasons for the apparent disagreement with experiment.

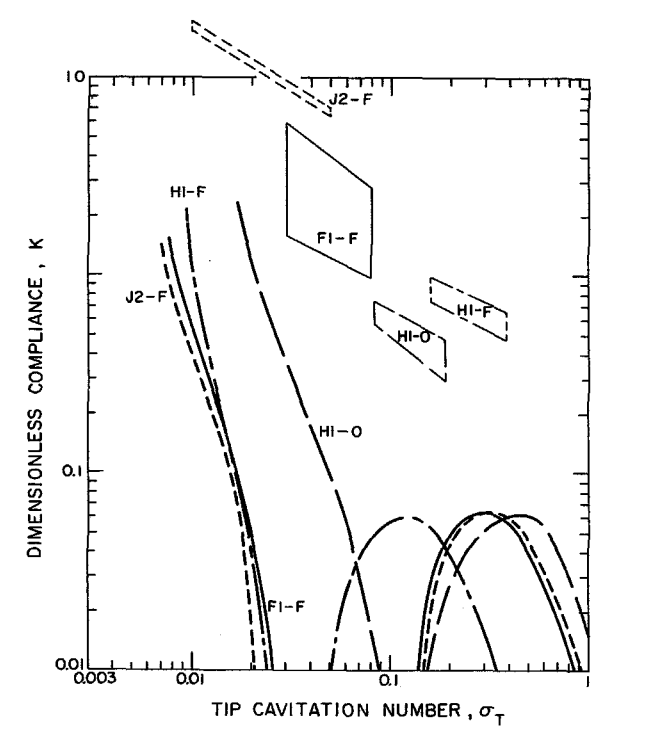

Fig. 11 Comparison of experimental derived K_B (boxes) with local tip compliance K_T^* (lines) for pumps J2-F, F1-F, H1-F and H1-0.

A) The question arises as to whether, as Ghahremani[10] maintains, the tip clearance leakage and resulting backflow would transport cavitation bubbles to the suction side of the pump in a sufficient number to create a backflow compliance which by dominating the blade compliance would make up the difference present in Figs. 9 and 10. It is to be expected that such an effect would be more marked for pumps whose inducer is relatively highly loaded; and indeed preliminary comparisons for the highly loaded inducers of the Titan pumps indicates an even greater discrepancy than found here for the Saturn pumps. Further analytical work on backflow compliance is clearly required to augment Ghahremani's[10] rough empirical calculations.

B) The validity of a quasistatic approach must also be questioned. The present authors consider that an appropriate reduced frequency, ω, might be

$$\omega = 2\pi f \cdot l_C / V_T$$

With f in the range 5 to 25 Hz, this yields values for ω in the Saturn pump experiments of between 0.02 and 0.3. It is notable that the values for J2 – F lie at the lower end of this range; yet J2 – F yields the largest values of compliance, K_B (Fig. 11). This suggests two alternative explanations: a) that the real, quasistatic compliance values are above the experimental curves in Figs. 9–11 and that K_B decreases with increasing ω; then the J2 – F line would be above the others since its ω is significantly smaller or b) that the models used to determine the experimental compliance inadvertently include inductive or resistive components which would cause the calculated compliance to be smaller than the real value, the reduction increasing with increasing ω.

C) While comparing the values in Fig. 11 it must be borne in mind that the deep minimums in the middle of the theoretical curves for K_T^* would most likely be eliminated during radial integration to find the theoretical K_B, as was the case for F1 – 0 and J2 – 0.

It is therefore clear that further progress in the analysis of turbopump cavitation compliance will require a) definitive experiments aimed at more direct measurement of compliance, b) theoretical analysis of unsteady, oscillatory flow, and c) further analyses of backflow and its contribution to compliance.

In summary, this paper presents a simple yet effective method of modifying existing linearized cavitating cascade theory in order to include the important effects of finite blade thickness and leading edge radius. The method clearly has applicability in turbopump analysis above and beyond its particular application in this paper.

References

[1] *Prevention of Coupled Structure-Propulsion Instability (POGO)*, NASA SP-8055, Oct. 1970.

[2] Rubin, S., "Longitudinal Instability of Liquid Rockets due to Propulsion Feedback (POGO)," *Journal of Spacecraft and Rockets*, Vol. 3, No. 8, Aug. 1966, pp. 1188–1195.

[3] Ghahremani, F. G., "Turbo-Pump Cavitation Compliance," Rept. TOR-0059(6531-01)-2, Sept. 1970, The Aerospace Corp., El Segundo, Calif.

[4] Acosta, A. J. and Hollander, A., "Remarks on Cavitation in Turbomachines," Rept. E-79.3, Oct. 1959, Engineering Science Dept., California Inst. of Technology, Pasadena, Calif.

[5] Cohen, H. and Sutherland, C. D., "Finite Cavity Cascade Flow," Mathematics Rept. 14, April 1958, Rensselaer Polytechnic Inst., Troy, N.Y.

[6] Acosta, A. J., "Cavitating Flow Past a Cascade of Circular Arc Hydrofoils," Rept. E-79.2, March 1960, Engineering Science Dept., California Inst. of Technology, Pasadena, Calif.

[7] Wade, R. B., "Linearized Theory of a Partially Cavitating Cascade of Flat Plate Hydrofoils," *Applied Scientific Research*, Vol. 17, No. 3, 1967, pp. 169–188.

[8] Stripling, L. B. and Acosta, A. J., "Cavitation in Turbopumps—Part I," *Transactions of the ASME, Ser. D; Journal of Basic Engineering*, Vol. 84, No. 3, Sept. 1962, pp. 326–338.

[9] Vaage, R. D., Fidler, L. E., and Zehnle, R. A., "Investigation of Characteristics of Feed System Instabilities," Interim Rept. MCR-71-278, Sept. 1971, Martin Marietta Corp., Denver, Colo.

[10] Ghahremani, F. G., "Pump Cavitation Compliance," *Cavitation Forum 1971*, ASME, New York, 1971, pp. 1–3.